Signature of large extra dimensions from *Z* boson pair production at the CERN Large Hadron Collider

Jun Gao, Chong Sheng Li,* Xiangdong Gao, and Jia Jun Zhang

Department of Physics and State Key Laboratory of Nuclear Physics and Technology, Peking University, Beijing 100871, China
(Received 17 March 2009; published 28 July 2009)

We study the *Z* boson pair production mediated by the Kaluza-Klein (KK) graviton in large extra dimensions (LED) at the CERN Large Hadron Collider (LHC). We use the partial wave unitarity to discuss the constraints on the process energy scale in order to give a self-consistent calculation. We find that the LED contributions can enhance the *Z* boson pair production cross sections significantly when the fundamental scale M_S of the large extra dimensions is up to several TeV. We also show that the kinematic distributions of the LED signals are greatly different from the standard model ones and the LHC can probe the M_S values up to 4.3–5.6 TeV at 3σ level depending on the number of the extra dimensions.

I. INTRODUCTION

The idea that quantum gravity can appear at the TeV energy scale well below the Planck mass $M_P \sim 1.2 \times 10^{19}$ GeV was proposed in the 1990s [1–3]. The large extra dimensions (LED) model [2] introduced by Arkani-Hamed, Dimopoulos, and Davli has attracted much attention as the presence of large extra dimensions brings a new solution to the hierarchy problem. In the LED model, *n* extra spatial dimensions are compactified on a torus with common circumference *R*, and a 3-brane is introduced in which the standard model (SM) particles live. The SM gauge interactions are confined to this brane and only the gravity can propagate in the extra dimensions. Then the four-dimensional Planck scale M_P is no longer the relevant scale but is related to the fundamental scale M_S as follows [4]:

$$M_P^2 \sim M_S^{n+2} R^n, \qquad (1)$$

where $M_S \sim$ TeV. According to Eq. (1), deviations from the usual Newtonian gravitational force law can be expected at distances smaller than $R \sim 2 \times 10^{-17+32/n}$ cm [4]. For $n \geq 2$, LED is consistent with the current experiments since gravitational forces currently are only well probed at distances about 40 μm [5] (However for $n = 2$, there are constraints arising from, e.g., supernova cooling [6], which require $M_S \gtrsim 14$ TeV if $n = 2$.) Recently, there are also some new constraints $M_S \gtrsim 1$ TeV [7] from a direct search at the Tevatron.

The gravitational couplings of the SM fields are given by

$$\int dx^4 \sqrt{-\hat{g}} \, \mathcal{L}_{SM}(\hat{g}, S, V, F), \qquad (2)$$

where $\hat{g}$ is the induced metric in four dimensions. Expanding $\hat{g}$ with the gravitational fields, we obtain

$$-\frac{\kappa}{2} \sum_{\vec{k}} \int dx^4 (\tilde{h}^{\mu\nu,\vec{k}} T_{\mu\nu} + \omega \tilde{\phi}^{\vec{k}} T^{\mu}{}_{\nu}), \qquad (3)$$

where $\kappa = \sqrt{16\pi}/M_P$, $\omega = \sqrt{2/(3n+6)}$, $T_{\mu\nu}$ is the energy-momentum tensor, and $\tilde{h}^{\mu\nu,\vec{k}}$, $\tilde{\phi}^{\vec{k}}$ are the four-dimensional Kaluza-Klein (KK) gravitons and KK scalars, respectively. From Eq. (3) it can be seen that the individual KK mode couples with a strength $1/M_P$ to the SM fields. However, since there are many KK modes, the total coupling strength is of the order $1/M_S$ after summing up all of them. For the phenomenology studies, we use the convention introduced in Ref. [8], where M_S is chosen to satisfy

$$\kappa^2 R^n = 8\pi(4\pi)^{n/2} \Gamma(n/2) M_S^{-(n+2)}. \qquad (4)$$

In this year, the LHC will start running and begin searching for the Higgs boson, further testing the SM, and also searching for new physics beyond the standard model. The *Z* boson pair production is an important process at the LHC and has been studied extensively. In the SM the *Z* boson pair can be produced directly through electroweak interactions with a total cross section of about 17 pb [9] at the LHC, corresponding to 1.7×10^6 events with an integrated luminosity of 100 fb^{-1}. With such a high production rate, it can serve as a probe for testing SM at TeV scale and also be an important background for new physics signals. Besides, the *Z* boson pair production can get additional contributions from new physics, for example, from the tree-level processes in extra dimension models [10,11], little Higgs model [12], and from loop level process in supersymmetry model [13], thus it can be used as a probe of new physics beyond standard model.

Usually, the most promising processes to test the LED model at the LHC are dilepton production, diphoton production, dijet production, and single vector boson or jet production associated with KK graviton [10,14]. However, the *Z* boson pair production also can be an important process especially for low M_S value, the total cross sections and invariant mass distributions of this process have

*csli@pku.edu.cn

been given in Ref. [10]. In this paper we will further study the Z boson pair production through the s-channel KK graviton exchange at the LHC. We focus on the four charged lepton final states and perform a Monte Carlo simulation to see the new physics effects on several kinematic distributions. Finally, we also show the LHC discovery potential of M_S with different values of n.

The arrangement of this paper is as follows. In Sec. II, we give the helicity amplitudes and discuss the unitarity constraints on the process energy scale. Section III shows the results of the total cross sections and Sec. IV contains the simulation results of several kinematic distributions and also the LHC reach of M_S. Section V is a brief conclusion.

II. HELICITY AMPLITUDES AND UNITARITY CONSTRAINTS

In the LED model the Z boson pair can be produced through KK graviton exchange from the gg fusion and $q\bar{q}$

annihilation, respectively, at the LHC. In order to calculate the relevant amplitudes we need to sum over all the KK graviton propagators,

$$D(s) = \sum_{\vec{k}} \frac{i}{s - m_{\vec{k}}^2 + i\epsilon}. \tag{5}$$

Since the KK graviton mass separation of $\mathcal{O}(1/R)$ is much smaller than all the other physical scales involved, we can obtain the above sum in the continuum limit [8],

$$D(s) = \frac{s^{n/2-1}}{\Gamma(n/2)} \frac{R^n}{(4\pi)^{n/2}} [\pi + 2iI(\Lambda/\sqrt{s})], \tag{6}$$

where $\Lambda \sim \mathcal{O}(M_S)$ is the explicit ultraviolet cutoff scale of the effective field theory, and

$$I(\Lambda/\sqrt{s}) = -\sum_{k=1}^{n/2-1} \frac{1}{2k}\left(\frac{\Lambda}{\sqrt{s}}\right)^{2k} - \frac{1}{2}\log\left(\frac{\Lambda^2}{s} - 1\right) \quad (n = \text{even})$$

$$= -\sum_{k=1}^{(n-1)/2} \frac{1}{2k-1}\left(\frac{\Lambda}{\sqrt{s}}\right)^{2k-1} + \frac{1}{2}\log\left(\frac{\Lambda + \sqrt{s}}{\Lambda - \sqrt{s}}\right) \quad (n = \text{odd}). \tag{7}$$

At the LHC the subprocess energy is comparable to M_S, so we need to keep all the terms in Eq. (7).

Since the scattering amplitudes grow quickly with $\sqrt{s}$, we should cut off the subprocess energy at some scale below Λ in order not to violate the unitarity. And we use the partial wave unitarity to discuss the constraint on $\sqrt{s}$. The J-partial wave amplitudes are given by

$$a^J_{\mu\mu'} = \frac{1}{64\pi} \int_{-1}^{1} d\cos\theta d^J_{\mu\mu'}(\cos\theta)[\mathcal{M}^{\lambda_1\lambda_2\lambda_3\lambda_4}], \tag{8}$$

where $\mu = \lambda_1 - \lambda_2$, $\mu' = \lambda_3 - \lambda_4$, θ is the scattering angle and $d^J_{\mu\mu'}$ is the Wigner function [15]. For the subprocess $gg \to ZZ$, the individual nonvanishing helicity amplitudes are

$$i\mathcal{M}_{+-+0} = -i\mathcal{M}_{+-0-} = 2\sqrt{2}i\delta_{cd}M_S^{-n-2}m_z\pi s^{(n+1)/2}(1 + \cos(\theta))\sin(\theta)\mathcal{A};$$

$$i\mathcal{M}_{+--0} = -i\mathcal{M}_{+-0+} = 2\sqrt{2}i\delta_{cd}M_S^{-n-2}m_z\pi s^{(n+1)/2}(1 - \cos(\theta))\sin(\theta)\mathcal{A};$$

$$i\mathcal{M}_{+-++} = i\mathcal{M}_{+---} = 4i\delta_{cd}M_S^{-n-2}m_z^2\pi s^{n/2}\sin^2(\theta)\mathcal{A}; \tag{9}$$

$$i\mathcal{M}_{+-+-} = 4i\delta_{cd}M_S^{-n-2}\pi s^{(n/2)+1}\cos^4(\theta/2)\mathcal{A};$$

$$i\mathcal{M}_{+--+} = 4i\delta_{cd}M_S^{-n-2}\pi s^{(n/2)+1}\sin^4(\theta/2)\mathcal{A};$$

$$i\mathcal{M}_{+-00} = -i\delta_{cd}M_S^{-n-2}\pi s^{n/2}(4m_z^2 + s)\sin^2(\theta)\mathcal{A},$$

where c, d are the gluon color indices and

$$\mathcal{A} = -2I(\Lambda/\sqrt{s}) + i\pi. \tag{10}$$

Since the energy scale we considered here is much larger than m_Z, so we can neglect all the terms that are proportional to m_Z. Then the main contributions arise from $\mathcal{M}_{+-+-}$, $\mathcal{M}_{+--+}$, and $\mathcal{M}_{+-00}$, and the only nonvanishing partial wave amplitudes correspond to the $J = 2$ partial

wave, which are given by

$$a^2_{2\pm2} = \frac{1}{40}\left(\frac{\sqrt{s}}{M_S}\right)^{n+2}\mathcal{A}, \qquad a^2_{20} = -a^2_{22}/\sqrt{6}. \tag{11}$$

All the above amplitudes a^2_{22}, a^2_{2-2}, and a^2_{20} contribute to the imaginary part of gg elastic scattering amplitudes according to the optical theorem, so the partial wave unitarity leads to
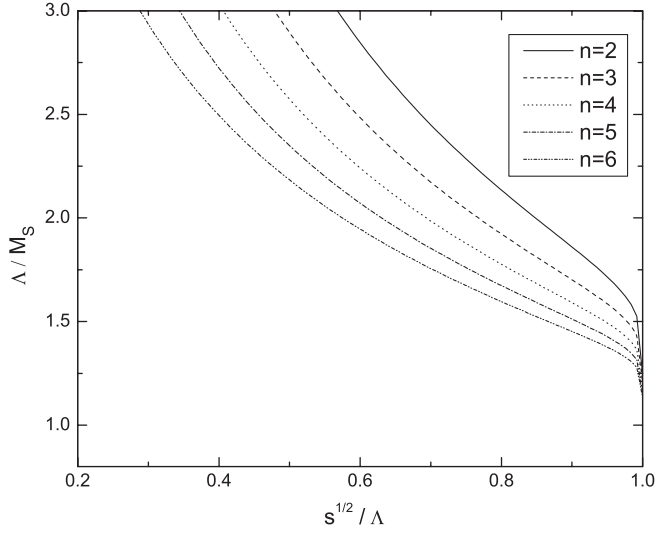
FIG. 1. Partial wave unitarity constraints on the ratios $\sqrt{s}/M_S$ and Λ/M_S; the allowed region is to the left of and below the curves.

$$|a_{22}^2|^2 + |a_{2-2}^2|^2 + |a_{20}^2|^2 < 1. \tag{12}$$

The partial wave amplitudes of $q\bar{q} \to ZZ$ lead to weaker constraints compared with the ones of $gg \to ZZ$, and are thus not shown here. In Fig. 1 we show the unitarity constraints on $\sqrt{s}$ with different Λ/M_S values according to Eq. (12). We can see that the constraints on $\sqrt{s}$ become

FIG. 2. The total cross sections of the Z boson pair production from LED contributions as functions of M_S at the LHC.

strong for large Λ/M_S values. In the following calculations we set $\Lambda = M_S$ and choose the energy cutoff to be $0.9M_S$ for simplicity, which is allowed by the unitarity constraints.

III. CROSS SECTION CALCULATIONS

The additional contributions to the partonic differential cross sections of the Z boson pair production in the LED model are given by

$$\frac{d\hat{\sigma}_{q\bar{q}}}{d\cos\theta} = \frac{\hat{s}\sqrt{1-4x}\,a^2(1+b^2)\mathcal{F}(n)\mathcal{T}(n)}{24}\left\{\frac{z^4(1-4x)^2 + 10z^2x(1-4x) - 2x(1-4x) - 1}{(1-z^2)(1-4x) + 4x^2}\right\}$$
$$+ \frac{\pi\hat{s}^3\sqrt{1-4x}\,\mathcal{F}^2(n)(\pi^2 + 4\mathcal{T}^2(n))}{384}\{-3z^4(1-4x)^2 + z^2(1-4x)(1-12x) + 2(1+4x)\}, \tag{13}$$

and

$$\frac{d\hat{\sigma}_{gg}}{d\cos\theta} = \frac{\pi\hat{s}^3\sqrt{1-4x}\,\mathcal{F}^2(n)(\pi^2 + 4\mathcal{T}^2(n))}{1024}$$
$$\times \{3z^4(1-4x)^2 + 2z^2(1-4x)(5+12x)$$
$$+ (1+12x)(3+4x)\}, \tag{14}$$

with

$$\mathcal{F}(n) = \hat{s}^{n/2-1}/M_S^{n+2}, \qquad \mathcal{T}(n) = I(M_S/\sqrt{\hat{s}}), \tag{15}$$

where $x = m_Z^2/\hat{s}$, $z = \cos\theta$, $a = e/(4\sin\theta_W\cos\theta_W)$, and $b = -1 + 8\sin^2\theta_W/3$ or $-1 + 4\sin^2\theta_W/3$, for up-type and down-type quark, respectively. Note that the factors $\mathcal{F}(n)$ and $\mathcal{T}(n)$ satisfy

$$\kappa^2 D(\hat{s}) = 8\pi\mathcal{F}(n)(\pi + 2i\mathcal{T}(n)). \tag{16}$$

In the numerical calculations we use the CTEQ6L1 PDF set [16] and choose the factorization scale to be the Z boson mass. To estimate the uncertainty of the tree-level calcu-
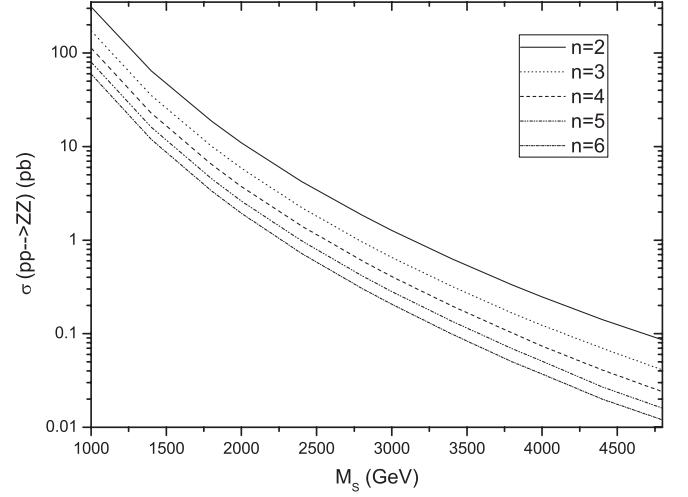
lations, we vary the factorization scale from m_Z to 1 TeV, and find that the uncertainty of the total cross section is about $\lesssim 50\%$, corresponding to a rather small shift of M_S. Figure 2 shows the total cross sections in the LED model as functions of M_S. We can see that the cross sections drop quickly with the increasing M_S, but can still reach hundreds of fb for $M_S = 4$ TeV. At low M_S values, the gg fusion channel is dominant, while for large M_S the $q\bar{q}$ annihilation contributions become important and are comparable to the ones of gg fusion channel.

IV. MONTE CARLO SIMULATIONS

We only consider the four charged leptons final state since at such high energy scale the two jets from highly boosted Z boson decay are hard to distinguish and the jet final states will suffer from large backgrounds also. The partonic level events are generated with COMPHEP 4.4 [17] and PYTHIA6.4 [18] is used to treat initial and final state radiations. We smear the energy and direction of the

charged leptons by a Gaussian distribution with the errors given by [19]

$$\Delta E_l / E_l = 0.1/\sqrt{E_l/\text{GeV}} \oplus 0.007,$$
$$\Delta \eta_l / \eta_l = \Delta \phi_l / \phi_l = 0.001. \tag{17}$$

Here we do not distinguish between electrons and muons for simplicity. We impose the basic acceptance cuts as follows [19]:

$$p_T^l > 15 \text{ GeV}, \quad |\eta_l| < 2.4, \quad \text{and} \quad \Delta R_{ll} > 0.1. \tag{18}$$

For the reconstruction of the two Z bosons we require the lepton combination of minimizing the following quantity

$$\Delta \equiv \sqrt{(m_{l_1 l_2} - m_Z)^2 + (m_{l_3 l_4} - m_Z)^2}. \tag{19}$$

In Figs. 3 and 4, we show the four lepton invariant mass distributions and the leading lepton p_T distributions, respectively. It can be seen that the LED signals prefer the

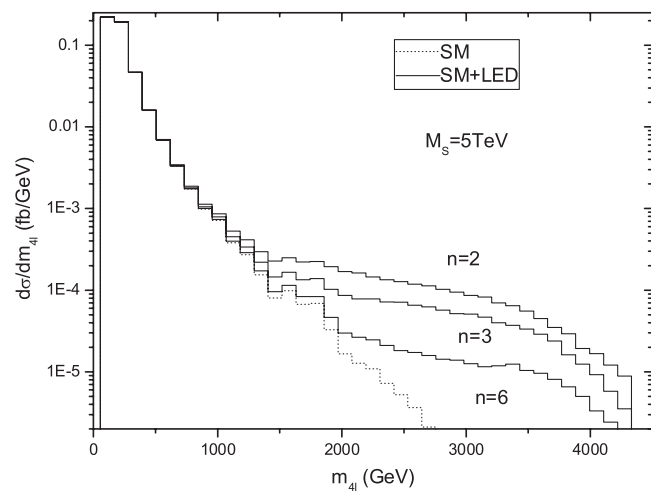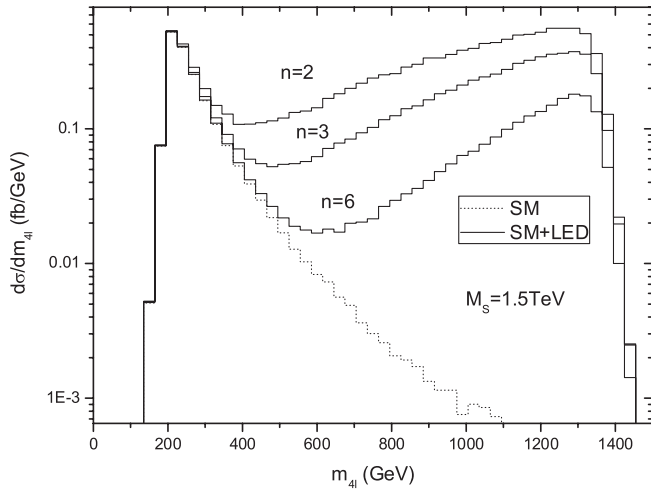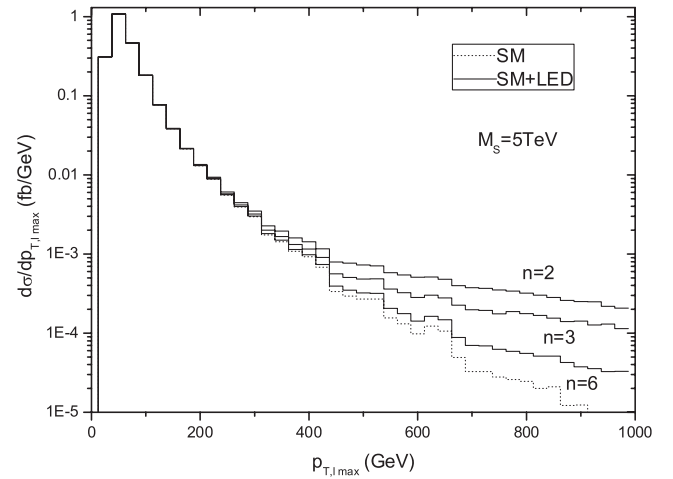FIG. 4. The transverse momentum distributions of the leading lepton.

FIG. 3. The invariant mass distributions of the four leptons.

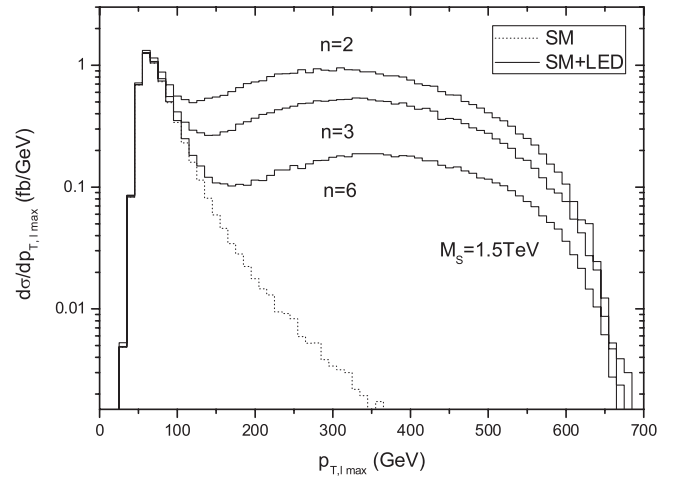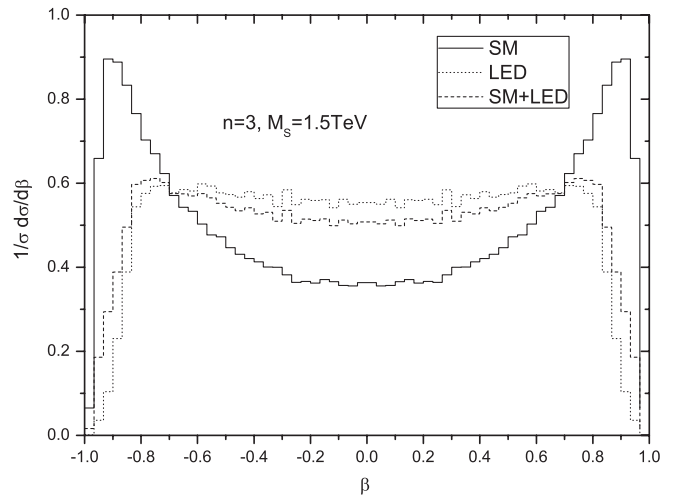

FIG. 5. The normalized velocity distributions of the rest frame of the Z pair.
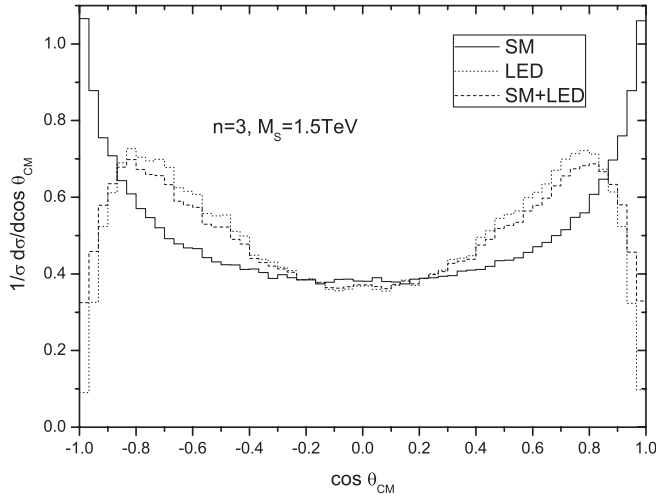
FIG. 6. The normalized polar angle distributions of the reconstructed Z boson in the rest frame of the Z pair.
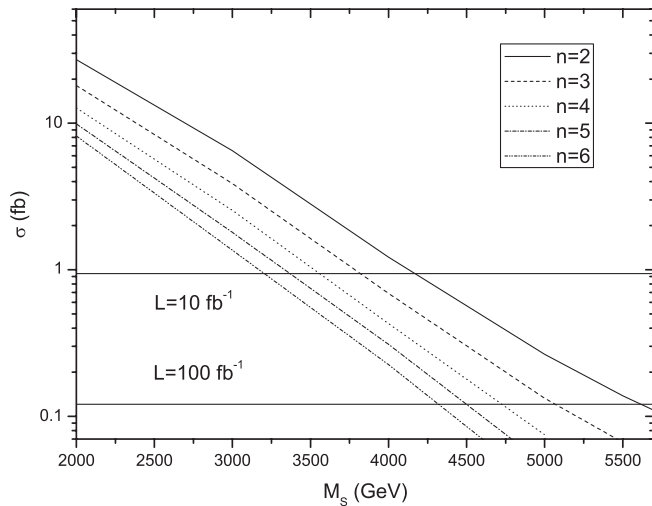

FIG. 7. The total cross sections of the LED signals after all the cuts as functions of M_S. The horizontal lines indicate the cross sections needed for a 3σ detection of the signal.

high invariant mass and high p_T regions. And for $M_S = 1.5$ TeV, the LED contributions can change the shape of the distributions significantly, while for $M_S = 5$ TeV, the changes of the distributions are relatively small, leading to long tails in the distributions. Figure 5 gives the velocity or

boost factor β distributions of the rest frame of the Z pair. We can see that the SM distribution will have two peaks in the forward and backward region since the Z boson pair can only be produced through $q\bar{q}$ annihilation in the SM. But for the LED contributions, gg fusion is dominant at low M_S values, thus the distribution will be flat and drop in both ends. In Fig. 6 we display the polar angle distributions of the reconstructed Z boson in the rest frame of the Z pair. Compared with the SM case, the LED signal falls down in both ends since the leptons from the decay of highly boosted Z boson in these regions fail the rapidity cut.

In order to further investigate the LHC reach of M_S, we introduce an invariant mass cut $m_{4l} > 1.5$ TeV and use a simple event counting method to calculate the signal significance. The Z boson pair production cross section in the SM is normalized to 17 pb based on the next-to-leading order result of Ref. [9]. Table I gives some results of the cut efficiencies, signal significance, and total cross sections after all the cuts. It can be seen that the invariant mass cut reduces the SM production rate significantly while only has a small influence on the LED signals, especially for large M_S values. In Fig. 7 we show the LED signal cross sections as functions of M_S after all the cuts, and also the LHC reach of M_S. Generally speaking, for the Z boson pair production process, the LHC can probe the M_S values up to 4.3–5.6 TeV for $n = 6$–2 at 3σ level, assuming an integrated luminosity of 100 fb^{-1}.

It should be noted that since we cut off the subprocess energy at some scale, we did not include the LED contributions beyond the cutoff in our calculations, because they depend on the unknown ultraviolet completion of the LED theory. For low M_S values, like $M_S = 1.5$ TeV, these contributions may be comparable or even larger than the ones we have considered, which may change the total cross sections and all the distributions. On the other hand, for high M_S values, like $M_S = 5$ TeV, the LED contributions beyond the cutoff are small due to the suppression of the parton distribution functions and the limited energy of the LHC, and can be neglected. So these contributions will not change the above results of LHC reach for M_S, which is about 5 TeV.

V. CONCLUSIONS

In conclusion, we have studied the Z boson pair production mediated by the KK graviton in large extra dimensions

TABLE I. Cut efficiencies, signal significance, and total cross sections after all the cuts with different parameters, assuming an integrated luminosity of 100 fb^{-1}.

Cut efficiency	$M_S = 2$ TeV			$M_S = 3$ TeV			$M_S = 4$ TeV			SM
	$n = 2$	$n = 3$	$n = 6$	$n = 2$	$n = 3$	$n = 6$	$n = 2$	$n = 3$	$n = 6$	
Basic cuts	0.73	0.73	0.76	0.76	0.78	0.79	0.72	0.74	0.75	0.35
$m_{4l} > 1.5$ TeV	0.25	0.30	0.42	0.51	0.59	0.66	0.49	0.56	0.61	0.000 27
Total cross section (fb)	27.2	18.1	8.2	6.49	3.87	1.36	1.22	0.69	0.22	0.046
$S/\sqrt{S + B}$	52	42	28	25	20	12	11	8.1	4.3	

at the LHC. Since the scattering amplitudes grow quickly with the energy, we used the partial wave unitarity to discuss the constraints on the process energy scale. We found that the LED contributions can enhance the Z boson pair production cross sections significantly when the fundamental scale M_S of the large extra dimensions is up to several TeV, and the kinematic distributions of the LED signals are greatly different from the SM ones through Monte Carlo simulations. Finally, we investigated the LHC reach of M_S and found that the LHC can probe the M_S values up to 4.3–5.6 TeV for $n = 6$–2 at 3σ level assuming an integrated luminosity of 100 fb^{-1}.

[1] I. Antoniadis, Phys. Lett. B **246**, 377 (1990); P. Horava and E. Witten, Nucl. Phys. **B460**, 506 (1996); E. Witten, Nucl. Phys. **B471**, 135 (1996); P. Horava and E. Witten, Nucl. Phys. **B475**, 94 (1996); J. D. Lykken, Phys. Rev. D **54**, R3693 (1996).

[2] N. Arkani-Hamed, S. Dimopoulos, and G. R. Dvali, Phys. Lett. B **429**, 263 (1998); I. Antoniadis, N. Arkani-Hamed, S. Dimopoulos, and G. R. Dvali, Phys. Lett. B **436**, 257 (1998); N. Arkani-Hamed, S. Dimopoulos, and G. R. Dvali, Phys. Rev. D **59**, 086004 (1999).

[3] L. Randall and R. Sundrum, Phys. Rev. Lett. **83**, 3370 (1999); **83**, 4690 (1999).

[4] C. Csaki, arXiv:hep-ph/0404096.

[5] D. J. Kapner et al., Phys. Rev. Lett. **98**, 021101 (2007).

[6] C. Hanhart, J. A. Pons, D. R. Phillips, and S. Reddy, Phys. Lett. B **509**, 1 (2001).

[7] V. Krutelyov (for the CDF and D0 Collaborations), arXiv:0807.0645.

[8] T. Han, J. D. Lykken, and R.-J. Zhang, Phys. Rev. D **59**, 105006 (1999).

[9] J. M. Campbell and R. K. Ellis, Phys. Rev. D **60**, 113006 (1999).

[10] D. Atwood, S. Bar-Shalom, and A. Soni, Phys. Rev. D **61**, 054003 (2000).

[11] S. C. Park, H. S. Song, and J.-H. Song, Phys. Rev. D **65**, 075008 (2002); P. K. Das, Phys. Rev. D **72**, 055009 (2005); K. Agashe, H. Davoudiasl, G. Perez, and A. Soni, Phys. Rev. D **76**, 036006 (2007).

[12] C. T. Hill and R. J. Hill, Phys. Rev. D **76**, 115014 (2007); A. Freitas, P. Schwaller, and D. Wyler, J. High Energy Phys. 09 (2008) 013; W.-Y. Keung, I. Low, and J. Shu, Phys. Rev. Lett. **101**, 091802 (2008).

[13] M. S. Berger and C. Kao, Phys. Rev. D **59**, 075004 (1999).

[14] G. F. Giudice, R. Rattazzi, and J. D. Wells, Nucl. Phys. **B544**, 3 (1999); JoAnne L. Hewett, Phys. Rev. Lett. **82**, 4765 (1999); C. Balazs, D. A. Dicus, H.-J. He, W. W. Repko, and C. P. Yuan, Phys. Rev. Lett. **83**, 2112 (1999); O. J. P. Eboli, T. Han, M. B. Magro, and P. G. Mercadante, Phys. Rev. D **61**, 094007 (2000); D. Atwood, S. Bar-Shalom, and A. Soni, Phys. Rev. D **62**, 056008 (2000); K.-m. Cheung and G. L. Landsberg, Phys. Rev. D **62**, 076003 (2000).

[15] C. Amsler et al. (Particle Data Group), Phys. Lett. B **667**, 1 (2008).

[16] J. Pumplin et al., J. High Energy Phys. 07 (2002) 012.

[17] E. Boos et al. (CompHEP Collaboration), Nucl. Instrum. Methods Phys. Res., Sect. A **534**, 250 (2004).

[18] T. Sjostrand, S. Mrenna, and P. Skands, J. High Energy Phys. 05 (2006) 026.

[19] G. L. Bayatian et al. (CMS Collaboration), Report No. CERN-LHCC-2006-001.